Large-Eddy Simulation of Turbulent Combustion

Heinz Pitsch

Department of Mechanical Engineering, Stanford University, Stanford, California 94305;
email: H.Pitsch@stanford.edu

Annu. Rev. Fluid Mech.
2006. 38:453–82

The *Annual Review of Fluid Mechanics* is online at
fluid.annualreviews.org

doi: 10.1146/annurev.fluid.38.050304.092133

0066-4189/06/0115-0453$20.00

Key Words

computational combustion, scalar mixing, scalar dissipation rate, nonpremixed combustion, premixed combustion

Abstract

Large-eddy simulation (LES) of turbulent combustion is a relatively new research field. Much research has been carried out over the past years, but to realize the full predictive potential of combustion LES, many fundamental questions still have to be addressed, and common practices of LES of nonreacting flows revisited. The focus of the present review is to highlight the fundamental differences between Reynolds-averaged Navier-Stokes (RANS) and LES combustion models for nonpremixed and premixed turbulent combustion, to identify some of the open questions and modeling issues for LES, and to provide future perspectives.

1. INTRODUCTION

The need for predictive simulation methods for turbulent reactive flows has led to a significant interest in large-eddy simulations (LES) in recent years. Technical combustion devices often require rapid mixing and short combustion times, yet must ensure proper flame stabilization. These conflicting requirements commonly lead to devices characterized by very complicated flow patterns, such as swirling flows, breakdowns of large-scale vortical structures, and recirculation regions. The accuracy required for predictions, for example, of pollutants in such flows typically cannot be achieved using Reynolds-averaged Navier-Stokes (RANS) simulations.

LES of turbulent combustion emerged as a science only in the 1990s and is hence a relatively new field. LES has already been applied to a variety of combustion problems of technical interest including predictions of pollutants (Eggenspieler & Menon 2004), aircraft engine combustion (Di Mare et al. 2004, Kim et al. 1999, Moin 2002), reciprocating engine combustion (Haworth & Jansen 2000), combustion, flashback, and blowoff in premixed stationary power-generation gas turbine combustors (Selle et al. 2004, Sommerer et al. 2004, Stone & Menon 2003), and combustion instabilities (Angelberger et al. 2000, Shinjo et al. 2003, Wall & Moin 2005). However, much of the necessary theory for combustion LES has yet to be developed, and its full predictive potential has not yet been reached. In the effort to develop this potential, it is important to realize that some properties of numerical algorithms, such as accuracy and energy conservation, important in LES of nonreactive flows, become even more important in LES of turbulent combustion.

In LES, the turbulent fields are separated into large-scale resolved and small-scale unresolved contributions. A spatial filtering operation applied to the instantaneous turbulent fields removes turbulent motions of length scales smaller than the filter size Δ. The governing equations for the remaining large-scale velocity field are amenable to discretization using a mesh with grid spacing of order Δ or smaller. This substantially reduces computational cost by a factor $\mathrm{Re}_\Delta^{9/4}$, where Re_Δ is the subfilter Reynolds number. However, just as with the RANS equations, there needs to be closure, for instance for the subfilter stresses. Many models have been provided for these quantities, and excellent reviews are given by Rogallo & Moin (1984), Lesieur & Métais (1996), and Meneveau & Katz (2000).

Although LES is a more computationally expensive technique than RANS, it offers two significant advantages. First, the large-scale motion of the turbulence that contains most of the turbulent kinetic energy and controls the dynamics of the turbulence is resolved, and hence computed directly. Second, knowledge of the large-scale dynamics and the assumption that an applied model should be valid independently of the filter size leads to the formulation of the so-called dynamic models (Germano et al. 1991, Moin et al. 1991), where model coefficients are determined as part of the solution.

Combustion in nonpremixed systems can only take place when fuel and oxidizer are mixed at a molecular level. Turbulent mixing increases the scalar variance, but only molecular diffusion forms a mixture that enables chemical reactions to occur. Similarly, in premixed combustion fuel and oxidizer are mixed, but at low temperature.

Again, turbulent mixing stirs the unburned mixture with hot combustion products, but only molecular transport increases the temperature of the reactants above the inner-layer temperature (Peters & Williams 1987), where self-sustained chemical reactions occur. Molecular mixing of scalar quantities, and hence chemical reactions in turbulent flows, occurs essentially on the smallest turbulent scales and is characterized and quantified by the dissipation rate of the scalar variance, which plays a central role in combustion modeling. As an example of the strong dependence of turbulent combustion on the small-scale mixing, it can easily be shown that for nonpremixed combustion in the limit of infinitely fast chemistry, the turbulent reaction rate is directly proportional to the scalar dissipation rate (Bilger 1976). For fast chemistry, the average chemical source term therefore follows a dissipation spectrum, and for typical LES of a high Reynolds number flow, there is no resolved part of the filtered reaction source term. This implies that for LES, as for RANS, the filtered chemical source term requires modeling. Hence, the two previously mentioned main advantages for LES apparently do not apply to the chemical source term.

The reason why LES still provides substantial advantages for modeling turbulent combustion is that the scalar mixing process is of paramount importance in chemical conversion. Nonreactive and reactive system studies show that LES predicts the scalar mixing process and dissipation rates with considerably improved accuracy compared to RANS, especially in complex flows. For example, to study the importance of turbulent scalar dissipation rate fluctuations on the combustion process and to highlight the differences between RANS and LES, Pitsch (2002) compared the results of two different LES simulations using unsteady flamelet models in which the scalar dissipation rate appears as a parameter. The only difference between the simulations was that only the Reynolds-averaged dissipation rate was used in one simulation (Pitsch & Steiner 2000a), whereas the other considered the resolved fluctuations of the filtered scalar dissipation rate predicted by LES. The results show substantially improved predictions, especially for minor species, when fluctuations are considered. Another such example is the simulation of a bluff-body stabilized flame (Raman & Pitsch 2005a), where a simple steady-state diffusion flamelet model (Peters 1984) in the context of an LES with a recursive filter refinement method led to excellent results. Such accuracy has not been achieved with RANS simulations of the same configuration (Kim & Huh 2002, Muradoglu et al. 2003). Both studies are discussed in more detail below. Similar arguments can be made for premixed turbulent combustion LES.

It is mentioned above that typically no portion of the filtered chemical source term can be resolved in LES, and that, as in RANS, combustion needs to be modeled entirely. Consequently, combustion models that have been proposed and applied in LES are mostly similar to RANS models. Different modeling approaches for RANS and their implementation are discussed in detail in the literature and in a large body of review articles (Janicka & Sadiki 2004; Klimenko & Bilger 1999; Peters 1984, 2000; Pope 1985; Veynante & Vervisch 2002). Although the basic ideas and fundamental concepts of RANS models can still be used for LES, turbulent combustion LES offers new modeling opportunities that can be explored and utilized, but also additional challenges that have to be addressed.

The focus of this review is to highlight the fundamental differences between RANS and LES combustion modeling, to identify some of the open questions and modeling issues, and to provide future perspectives. Therefore, the underlying modeling concepts are reviewed only briefly. In combustion modeling, a distinction is often made between models for premixed and nonpremixed combustion. Although this distinction is not truly applicable to most technical combustion systems, it is advantageous for the purpose of the present paper. Therefore, first nonpremixed and then premixed combustion LES are discussed, with the caveat that some of the models might actually be applicable in both regimes, at least to some extent.

2. LES OF NONPREMIXED TURBULENT COMBUSTION

2.1. Overview

In nonpremixed combustion, fuel and oxidizer are initially separated. Chemical reactions occur only because of diffusive molecular mixing of these components. If the chemistry is fast enough, a reaction layer forms at approximately stoichiometric conditions. In this layer, fuel and oxygen are consumed and reaction products are formed. For hydrogen and hydrocarbon chemistry in engineering devices, combustion is typically controlled by the rate of molecular mixing, although the chemistry becomes important if the chemical timescale compares with the timescale of the turbulence. In that case, local flame extinction might occur. Also, the chemistry of pollutant formation is often governed by slow chemical reactions.

In RANS modeling it has long been realized that the direct closure of the mean chemical source term in the averaged species transport equations can hardly be accomplished, and conserved scalar methods have been used in many applications. Using so-called coupling functions, the rate of mixing of fuel and oxidizer can be described by a nonreactive scalar, the mixture fraction. Different definitions have been used for the mixture fraction (Bilger 1976, Pitsch & Peters 1998), but essentially the mixture fraction is a measure of the local equivalence ratio. Hence, the mixture fraction is a conserved scalar, independent of the chemistry. This leads to the so-called conserved scalar method, which forms the basis for most of the combustion models for nonpremixed turbulent combustion. Considering the simplest case of infinitely fast chemistry, all species mass fractions and the temperature are a function of mixture fraction only. If the subfilter probability distribution of the mixture fraction is known, the Favre-filtered mass fractions $\tilde{Y}_i$, for instance, can then be obtained as

$$\tilde{Y}_i = \int_0^1 Y_i(Z) f(Z)\, dZ, \tag{1}$$

where Z is the mixture fraction and $f(Z)$ is the marginal density-weighted filter probability density function (FPDF) of the mixture fraction. Applications of simple conserved scalar models in LES have been based on infinitely fast irreversible chemistry (Pierce & Moin 1998) and equilibrium chemistry (Cook & Riley 1994).

The flamelet model and the conditional moment closure (CMC) model are conserved scalar models that account for finite-rate chemistry effects. Many models that

have been formulated for LES are variants of these and some are discussed below. These models essentially provide state relationships for the reactive scalars as functions of mixture fraction and other possible parameters, such as the scalar dissipation rate. Filtered quantities are then obtained by a relation similar to Equation 1, but using a presumed joint FPDF of the mixture fraction and, for example, the scalar dissipation rate.

Because the probability density function (PDF) plays a central role in most models for nonpremixed combustion, it is necessary to emphasize the special meaning of the FPDF in LES. Here, the example of the marginal FPDF of the mixture fraction is discussed, but similar arguments can be made for the joint composition FPDF. In Reynolds-averaged methods, a one-point PDF can be determined by repeating an experiment many times and recording the mixture fraction at a given time and position in space. For a sufficiently large number of samples, the PDF of the ensemble can be determined with good accuracy. In LES, assuming a simple box filter, the data of interest is a one-time, one-point probability distribution in a volume corresponding to the filter size surrounding the point of interest. If an experimentally observed spatial mixture fraction distribution is considered at a given time, the FPDF cannot simply be evaluated from these data, because the observed distribution is characteristic of this particular realization and it is not a statistical property. As a statistical property, the FPDF must be defined by an ensemble that can potentially have an arbitrary large number of samples. In the context of transported PDF model formulations for LES, which are discussed below, Pope (1990) introduced the notion of the filtered density function (FDF), which describes the local subfilter state of the considered experiment. The FDF is not an FPDF, because it describes a single realization. The FPDF is defined only as the average of the FDF of many realizations given the same resolved field (Fox 2003). It is important to distinguish between the FDF and the FPDF, especially in using direct numerical simulation (DNS) data to evaluate models, and in the transported FDF models discussed below. Only the FDF can be evaluated from typical DNS data, whereas the FPDF is required for subfilter modeling.

For conserved scalar models, a presumed shape of the FPDF has to be provided. Similar to RANS models, a beta-function distribution is usually assumed for the marginal FPDF of the mixture fraction, and parameterized by the first two moments of the mixture fraction. The filtered mixture fraction is determined by the solution of a transport equation, whereas algebraic models are mostly used for the subfilter scalar variance. The beta-function is expected to be a better model for the FPDF in LES than for the PDF in RANS, because the FPDF is generally more narrow, and hence the exact shape is less important. It can also be expected that intermittency, which is a main source of error when using the beta-function in RANS, will mostly occur on the resolved scales. The validity of the beta-function representation of the FPDF of the mixture fraction has been investigated by several authors using DNS data of nonpremixed reacting flows of both constant and variable density (Cook & Riley 1994, Jimenez et al. 1997, Wall et al. 2000). The main conclusion of these studies is that the beta-function distribution provides a good estimate for the FPDF of the mixture fraction and that this estimate is even better in LES than in RANS models. Furthermore, the model is particularly good when evaluated using the mixture fraction variance

taken from DNS data, suggesting that the beta-function as a model for the statistical distribution of the mixture fraction performs much better than the commonly used subgrid-scale models for the mixture fraction variance. However, recent studies by Tong (2001) and Tong et al. (2005) show that the FPDF often substantially deviates from the beta-function. This is discussed in more detail below.

In the following, different variants of the flamelet model, the CMC model, and the transported FDF model are discussed in more detail. Because all such models require the scalar dissipation rate, modeling of this quantity is discussed first.

2.2. Modeling the Scalar Dissipation Rate

Although different conceptual ideas and assumptions are used in the combustion models discussed here, most of them need a model for the scalar dissipation rate. The dissipation rate of the mixture fraction is a fundamental parameter in nonpremixed combustion, which determines the filtered reaction rates, if combustion is mixing controlled. High rates of dissipation can also lead to local or global flame extinction. Models based on presumed FPDFs also require a model for the subfilter scalar variance. Here, the most commonly used model formulations for LES are reviewed briefly, differences with the typical RANS models are pointed out, and potential areas of improvement are discussed.

An illustration of the importance of the scalar variance and dissipation rate in LES of nonpremixed combustion modeling is given by the following example. Pope (2004) pointed out that LES is an incomplete model if the filter size can be arbitrarily specified. This is an important issue, especially for combustion LES, because of the importance of the subfilter models. To fix the arbitrariness of the filter, Raman & Pitsch (2005a) proposed a recursive filter refinement method, where the local filter width is determined such that the ratio of subfilter scalar variance to the maximum possible variance is smaller than a specified value. The maximum possible variance can be expressed in terms of the resolved mixture fraction as $\tilde{Z}(1-\tilde{Z})$. It was demonstrated in the simulation of a bluff-body stabilized flame that this method better resolves high scalar variance and dissipation regions, which leads to significant improvement in results. Some of these results are shown in **Figure 1**.

In RANS models, typically a transport equation is solved for the scalar variance $\langle Z''^2 \rangle$, in which the Reynolds-averaged scalar dissipation rate $\langle \chi \rangle$ appears as an unclosed sink term that requires modeling. The additional assumption of a constant ratio of the integral timescale of the velocity τ_t and the scalar fields leads to the expression

$$\langle \chi \rangle = c_\phi \frac{1}{\tau_t} \langle Z''^2 \rangle, \tag{2}$$

where c_ϕ is the so-called timescale ratio.

In the models most commonly used in LES (Girimaji & Zhou 1996, Pierce & Moin 1998), the scalar variance transport equation and the timescale ratio assumption are actually used in the opposite sense. Instead of solving the subfilter variance equation, the assumption that the scalar variance production appearing in that equation equals the dissipation term leads to an algebraic model for the dissipation rate of the form

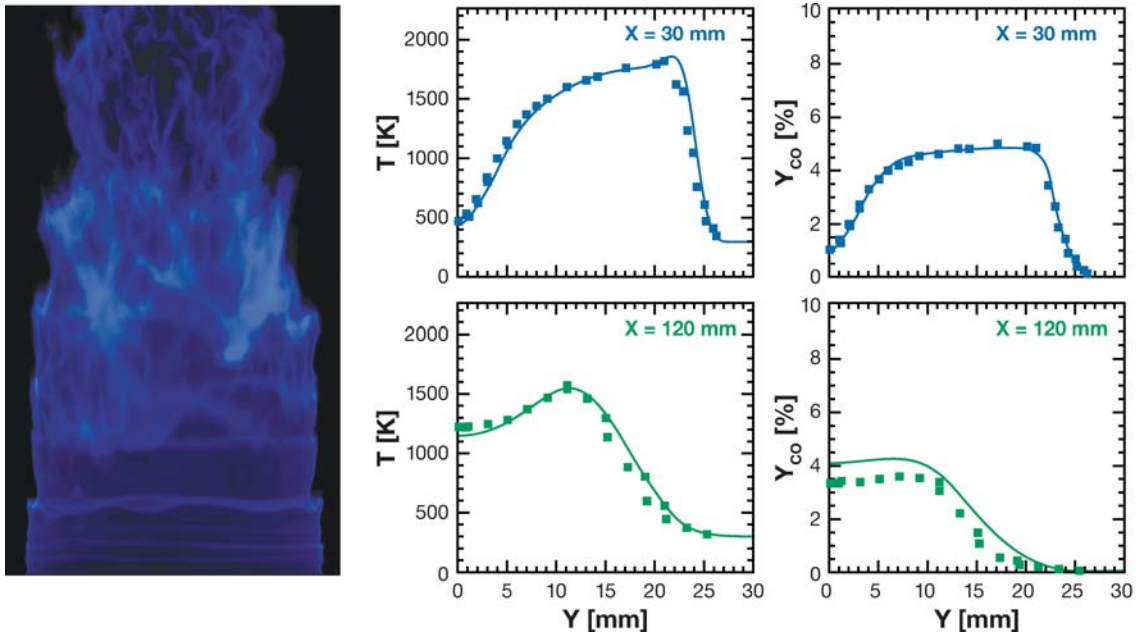

Figure 1

Results from large-eddy simulation of the Sydney bluff-body flame (Raman & Pitsch 2005a). Flame representation from simulation results (*left*) and time-averaged radial profiles of temperature and CO mass fraction at $x = 30$ mm and $x = 120$ mm, which are in and downstream of the recirculation region, respectively. The left figure shows computed chemiluminescence emissions of CH collected in an observation plane with a ray tracing technique (M. Hermann, private communication). Experimental data are taken from Dally et al. (1998).

$$\tilde{\chi} = 2 D_t \left(\nabla \tilde{Z}\right)^2, \tag{3}$$

where an eddy diffusivity model was used for the subfilter scalar flux in the production term. $D_t = (c_Z \Delta)^2 \tilde{\mathcal{S}}$ is the eddy diffusivity, where c_Z can be determined using a dynamic procedure and $\tilde{\mathcal{S}} = |2\tilde{S}_{ij}\tilde{S}_{ij}|^{1/2}$ is the characteristic Favre-filtered rate of strain. Writing Equation 2 for the subfilter scales and combining it with Equation 3 then leads to the model for the scalar variance

$$\widetilde{Z''^2} = c_V \Delta^2 \left(\nabla \tilde{Z}\right)^2, \tag{4}$$

where $\tau_{t,\Delta} \sim 1/\tilde{\mathcal{S}}$ is assumed, and a new coefficient c_V is introduced, which can be determined dynamically following Pierce & Moin (1998). From Equations 2 and 3, and the dynamically determined coefficients of the eddy diffusivity and the scalar variance, the timescale ratio c_ϕ can be determined as $c_\phi = 2c_Z^2/c_V$.

Alternative models for LES, where a transport equation for the scalar variance is solved, have also been proposed (Jiménez et al. 2001). It seems that then the production/dissipation balance assumption would not be required, but this is not the case. The assumption of constant timescale ratio still has to be made and an equation of

the form of Equation 2 implicitly assumes that production equals dissipation. This is because the dissipation rate can only be used in evaluating the timescale at the filter scale, if the scale invariance assumption is made for the scalar dissipation rate. This assumption implies that production is equal to dissipation.

Although the production/dissipation balance assumption seems to be inherently used in all models for the dissipation rate, there is strong evidence that it is not always applicable, which might have severe consequences for turbulent combustion modeling. Tong (2001) showed from filtering experimental data in nonreactive jets that the occurrence of so-called ramp-cliff structures leads to locally high scalar dissipation rates and bi-modal subfilter distributions of the conserved scalar, which cannot be described by the beta-function distribution. Because the ramp-cliff structures are a direct result of the large-scale turbulent motion, and not of the energy cascade, they cannot be described by the production/dissipation balance assumption. More recently, the same conclusions were found by analyzing experimental data of a jet diffusion flame (Tong et al. 2005). Although the bi-modal FDFs are observed with a low probability (roughly 15% in the diffusion flame experiment at $x/D = 15$), because of the locally high dissipation rates, these might be very important for the dynamics of the flame structure. This also indicates that the accuracy of mixing models used in transported FDF models in LES is very important.

Another complication of using models for scalar variance and dissipation rate in LES is of numerical nature. It is common practice in nonreactive, as in combustion, LES to use implicit filtering, which means that the filter is given by the numerical grid spacing. It follows that the smallest resolved scales are actually under-resolved. Because of numerical diffusion, the energy content of these scales is underpredicted. For nonreactive LES, this is usually less important, because the flow dynamics are mostly governed by the large scales of the turbulence. For reactive flows this is different: As shown by Equations 3 and 4, the models for scalar dissipation rate and variance depend on the square of the resolved scalar gradient. This quantity, however, is largest on the smallest resolved scales. Similarly, the production term in the scalar variance equation depends on the same quantity, and therefore the solution of the scalar variance equation also underpredicts the scalar variance. Consequently, models of the form of Equation 3 or 4, or models involving the subfilter variance transport equation, should only be used with explicit filtering or numerical schemes of higher-order accuracy.

Clearly, there is a need for new modeling approaches for scalar variance and dissipation rate that account for the small-scale structure of the scalar field.

2.3. Models for Nonpremixed Combustion LES

2.3.1. Steady and unsteady flamelet models. Flamelet models for nonpremixed combustion were introduced by Peters (1983, 1984). The basic assumption is that the chemical timescales are short enough that reactions occur in a thin layer around stoichiometric mixture on a scale smaller than the small scales of the turbulence. This has two consequences: The structure of the reaction zone remains laminar, and diffusive transport occurs essentially in the direction normal to the surface of

stoichiometric mixture. Then, the scalar transport equations can be transformed to a system where the mixture fraction is an independent coordinate. A subsequent asymptotic approximation leads to the flamelet equations,

$$\frac{\partial Y_i}{\partial \tau} - \rho \frac{\chi}{2} \frac{\partial^2 Y_i}{\partial Z^2} - \dot{m}_i = 0, \tag{5}$$

where τ is the time, ρ is the density, and $\dot{m}_i$ are the chemical production rates. Similar equations can be derived for other scalars such as temperature. The steady laminar flamelet model is developed by assuming the flame structure is in steady state. Then, the time derivative in Equation 5 can be neglected. The solution is then only a function of the scalar dissipation rate and the boundary conditions, and can be precomputed and tabulated in terms of these quantities. This model was considered in some of the early a priori studies of LES combustion models (Cook & Riley 1998, De Bruyn Kops et al. 1998) and has also been successfully applied in simulations of experimental configurations (Kempf et al. 2003, Raman & Pitsch 2005a).

The steady flamelet model is often used, especially in LES, because of its simplicity and considerable improvements over fast chemistry assumptions. However, the steady-state assumption is inaccurate if slow chemical or physical processes have to be considered (Pitsch et al. 1998). Examples of such processes include the formation of pollutants and radiative heat transfer. In these cases, the full unsteady equations should be solved.

Pitsch & Steiner (2000a,b) used the Lagrangian flamelet model (LFM) (Pitsch et al. 1998) as a subfilter combustion model for LES in an application to a piloted methane/air diffusion flame (Barlow & Frank 1998) using a 20-step reduced chemical scheme based on the GRI 2.11 mechanism (Bowman et al. 1995). The unsteady flamelet equations are solved coupled with the LES solution to provide the filtered density and other filtered scalar quantities using a presumed FPDF of the mixture fraction. The scalar dissipation rate required to solve Equation 5 is determined from the LES fields as a cross-sectional conditionally averaged value using a model similar to the conditional source term estimation method by Bushe & Steiner (1999), which is described below. The unconditional scalar dissipation rate was determined from a dynamic model (Pierce & Moin 1998). This study is the first demonstration of combustion LES of a realistic configuration using a detailed description of the chemistry. The results are promising, especially for NO, but because of the cross-sectional averaging of the scalar dissipation rate, local fluctuations of this quantity are not considered and the potential of LES is not fully realized. Also, this model cannot be easily applied in simulations of more complex flow fields. In a more recent formulation, the Eulerian flamelet model (Pitsch 2002), the flamelet equations are rewritten in an Eulerian form, which leads to a full coupling with the LES solver, and thereby enables the consideration of the resolved fluctuations of the scalar dissipation rate in the combustion model. Examples of the results are shown in **Figure 2**. The resolved scalar dissipation rate field is dominated by features occurring on the large scale of the turbulence. Layers of high dissipation rate alternate with low dissipation rate regions. In the LFM results, as well as in several earlier RANS-type modeling studies (Barlow 2000), where these fluctuations are not considered, some heat

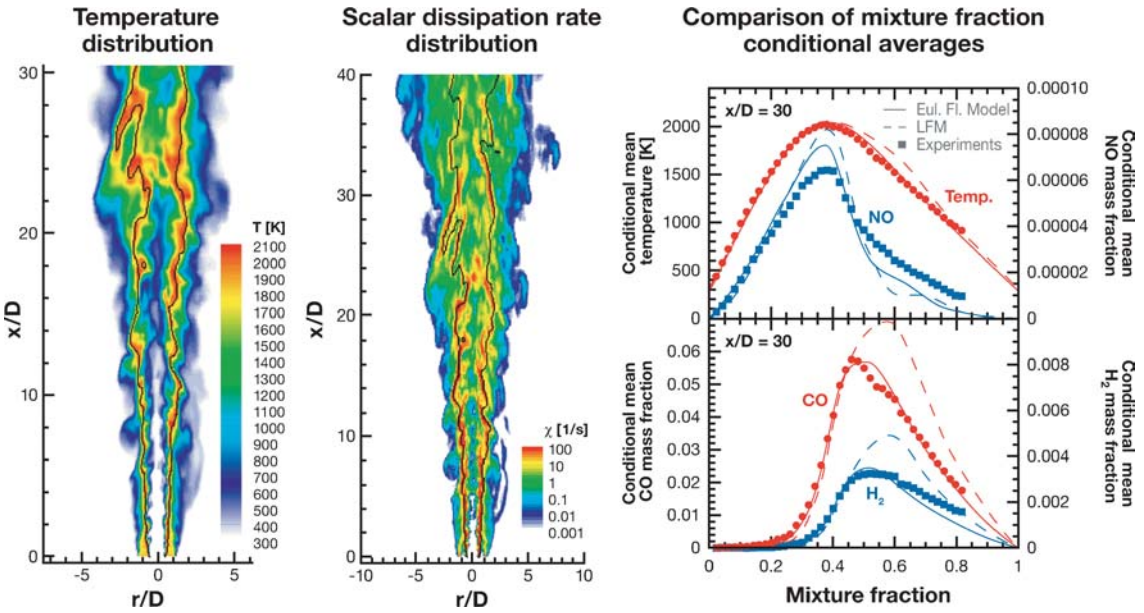

Figure 2

Results from large-eddy simulation of Sandia flame D (Pitsch 2002, Pitsch & Steiner 2000a) using the Eulerian flamelet model (*solid lines*) and the Lagrangian flamelet model (*dashed lines*) compared with experimental data of Barlow & Frank (1998). Temperature distribution (*left*), scalar dissipation rate distribution (*center*), and comparison of mixture fraction–conditioned averages of temperature and mass fractions of NO, CO, and H_2 at $x/D = 30$.

release occurs on the rich partially premixed side of the flame, which leads to strong CO formation in these regions. Accounting for the richness of the predicted spatial distribution of the scalar dissipation rate substantially improves the comparison with the experimental data by suppressing the heat release in the rich regions, and hence the formation of CO.

2.3.2. Flamelet/Progress variable method. A model that was developed specifically for LES is the flamelet/progress variable model (FPV) by Pierce & Moin (2001, 2004). The model uses a steady-state flamelet library, but is substantially different from the typical steady laminar flamelet model (SLFM) used by others (Branley & Jones 2001, Cook & Riley 1998, De Bruyn Kops et al. 1998, Kempf et al. 2003). Instead of using the scalar dissipation rate as a parameter in the flamelet library, the reaction progress variable is used for the parameterization. A transport equation is solved for the filtered reaction progress variable, which can, for example, be defined as the sum of the mass fractions of CO_2, H_2O, CO, and H_2. The filtered chemical source term in this transport equation is closed using the flamelet library and a presumed joint FPDF of mixture fraction and reaction progress variable. The advantage of this different way of parameterizing the flamelet library is that it potentially gives a better description of local extinction and reignition phenomena and of flame

liftoff. Steady-state solutions of Equation 5 exist for all possible values of the reaction progress variable below the equilibrium value and can be used in the flamelet library. For higher scalar dissipation rates, the reaction progress variable becomes smaller because of diffusive effects until extinction occurs, where the solution jumps to the nonburning state. If the scalar dissipation rate is used in the parameterization, only the burning solutions are available.

One challenge of using the reaction progress variable is that, in order to close the model, the joint FPDF of mixture fraction and reaction progress variable needs to be provided. In the application of the model to a nonpremixed dump combustor geometry by Pierce & Moin (2001, 2004), a delta-function was used for the FPDF of the reaction progress variable. Comparison with experimental data demonstrated substantial improvement of the predictions compared with SLFM, caused by a more accurate description of the flame stabilization region. The FPV model can be interpreted as a two-variable intrinsically low dimensional manifold (ILDM) model (Maas & Pope 1992), where the ILDM tabulation is generated with a flamelet model.

In a priori tests using data from DNS of nonpremixed combustion in isotropic turbulence (Sripakagorn et al. 2004), Ihme et al. (2004) investigated potential areas for improvement of the FPV model. The model for the presumed FPDF for the reaction progress variable was identified as important. It was also found that the steady-state assumption of the flamelet solutions, especially during reignition at low scalar dissipation rate, is inaccurate. The beta function was proposed as a possible improvement for the reaction progress variable FPDF, and a closure model for the reactive scalar variance equation was provided. New developments include the evaluation and application of the statistically most likely distribution (Pope 1979) as a new model for the reactive scalar FPDF (Ihme & Pitsch 2005), and the extension of the model to an unsteady flamelet library formulation (Pitsch & Ihme 2005).

2.3.3. Conditional moment closure. In the CMC model, originally proposed in a RANS context by Klimenko (1990) and Bilger (1993), transport equations are derived for mixture fraction–conditioned averages of the reactive scalars. The resulting equations are dependent on time, three spatial dimensions, and the mixture fraction. The mixture fraction conditioning greatly simplifies the modeling of the averaged chemical source term, but makes it difficult to solve these equations in LES. Kim & Pitsch (2005) formulated the CMC model for LES. Models are provided for all unclosed terms, and most of the models are tested using DNS data. Also, a lower-dimensional model is developed and tested, where the number of independent spatial coordinates was reduced by integrating the reactive scalar transport equations in one direction. For first-order closure, this model is very similar to the Eulerian flamelet model (Pitsch 2002). Higher-order closure changes the modeling of the unclosed terms in the CMC model, whereas in the Eulerian flamelet model, ensembles of flamelets would be computed simultaneously. For an application of the full CMC model in LES of a practical configuration, several issues regarding boundary conditions and numerical efficiency are important and have to be addressed (Bilger et al. 2005, Kim & Pitsch 2005).

Another interesting formulation of the CMC model for LES is the so-called conditional source term estimation model by Bushe & Steiner (1999). Here, transport

equations are solved for all reactive scalars appearing in the applied chemical scheme. The chemical source terms are closed using the conditionally averaged scalar values and the mixture fraction FPDF. The CMC concept is used to determine the conditionally filtered scalars from the unconditional values obtained from the solution of the transport equations. For this, the integrals of the form of Equation 1 are inverted for a certain region of the flow field using the presumed mixture fraction FPDF and assuming homogeneous statistics in that region. It is apparent that the model cannot be used for radical species, which peak in thin layers on the subfilter scale. It is also important that the assumption of statistical homogeneity, which is used in the deconvolution, has to be restricted to regions smaller than the large scales of the turbulence, because, otherwise, the full potential of LES is again not realized.

2.3.4. Transported FDF models. The transported joint scalar and joint scalar/velocity PDF method has been applied to turbulent reacting flows using RANS methods in many studies (Chen et al. 1989, Pope 1985, Saxena & Pope 1998, Xu & Pope 2000), and has also been extended to LES by using the FDF originally introduced by Pope (1990) and further studied and extended by Gao & O'Brien (1993), Colucci et al. (1998), Sheikhi et al. (2003), and others. The transport equation for the one-point one-time joint FDF of all reactive scalars and temperature or enthalpy is given by

$$\frac{\partial F}{\partial t} + \nabla \cdot (\tilde{\mathbf{v}} F) + \nabla \cdot (\widetilde{\mathbf{v}'|\psi} F) = -\frac{\partial}{\partial \psi}\left[\left(\frac{1}{\tilde{\rho}}\overline{\nabla \cdot \rho D \nabla \phi|\psi} + \mathbf{S}(\psi)\right) F\right], \qquad (6)$$

where $F(\psi)$ is the density-weighted FDF, t is the time, $\mathbf{v}$ is the velocity, ϕ and ψ are the vector of scalars and its sample space representation, respectively, and D is the molecular diffusivity. The tilde stands for mass weighted, the overline for conventional filtering, and the prime for a fluctuation. In Equation 6, the chemical source term $\mathbf{S}(\psi)$ appears in closed form. Molecular mixing, however, depends on multipoint information and therefore has to be modeled. This is a severe restriction of the transported FDF models for applications in combustion, where transport is usually rate controlling, and hence more important than the details of the chemistry. Because molecular mixing occurs on the smallest scales, the mixing models used in LES so far are the same as those developed for RANS.

The joint scalar FDF depends on space, time, and all independent scalars. Therefore, the FDF transport equation cannot be solved using finite-volume or finite-difference methods and is commonly represented by an equivalent system of notional particles. For each particle, ordinary differential equations are solved for particle motion, temperature or enthalpy, and species mass fractions (Pope 1985). Because the accuracy of the method scales with the square root of the number of notional particles, typically a large number of particles per cell is required. If the error of the method with only one particle per cell is estimated to be the root mean square of the described quantity, then 100 particles per cell are required to achieve an error on the order of 10% of the root mean square (RMS). For RANS simulations of statistically stationary problems, good statistics can be achieved by collecting large ensembles of particles over time.

The main challenges in applying FDF methods in LES are the computational cost and the formulation of robust and consistent algorithms. Because of the inherent unsteadiness in LES, the requirement of statistical convergence has to be satisfied at each time step. For an LES with 2 million cells and 100 particles per cell, approximately 200 million particles are required. For each of these particles, the equations for the species mass fractions have to be solved. Especially the integration of the chemical source terms is very time consuming and renders the FDF method in LES virtually impossible without special treatment of the chemical source terms. Pope (1997) proposed the in situ adaptive tabulation (ISAT) method for the chemical source term integration, and has demonstrated substantially reduced integration times for applications in RANS. The assessment and algorithmic optimization of the method in LES was recently initiated by Lu et al. (2004).

To reduce the cost of FDF/LES, it is desirable to use a small number of particles per cell. Applications of the FDF method in LES show that if a practical number of 50 particles per cell is used, large fluctuations in the filtered density occur because of statistical errors, causing problems for numerical solvers. Muradoglu et al. (1999) proposed a hybrid scheme, which considerably improves the robustness of the method. Here, a transport equation for the energy is solved. The chemical source term in that equation is evaluated from the joint PDF, which can be evaluated from the particles. Using this method, the filtered density can be evaluated in three different fashions: from the particle weights, which are assigned at the beginning of the simulation and which are fixed in time; from the joint composition FDF; and from the solution of the energy equation. It is important to ensure time-accurate consistency of these densities throughout the simulation. Zhang & Haworth (2004) have provided an appropriate algorithm for unsteady RANS. For LES, more work is still required.

Applications of the transported FDF method to realistic flame geometries have mostly been restricted to solving for the FDF of the mixture fraction in combination with the laminar flamelet model (Raman et al. 2005, Sheiki et al. 2005). However, although the application of the transported FDF method substantially increases computational times, the feasibility of the method for LES has been demonstrated in simulations of the Sandia flames D and E with a reduced 17-step mechanism based on the GRI-2.11 mechanism (Raman & Pitsch 2005b). These simulations used a mesh of approximately 3 million computational cells. For mixing, the interaction-by-exchange-with-the-mean (IEM) model was employed with the timescale ratio determined from a dynamic model. Results for flame E, where local extinction and reignition is important, are shown in **Figure 3**. The conditional averages show that, because of local extinction, unreacted molecular oxygen remains even at stoichiometric conditions ($Z_{st} = 0.35$). Comparisons for other species show generally good agreement, but the CO mass fraction, for instance, is overpredicted at rich conditions. Extinguished parts of the flame can also be seen in the instantaneous temperature field given for flame E.

Finally, note that usually in applications of transported FDF methods in LES the difference between the FDF, as a description of a single subfilter realization, and the FPDF, as the probability of finding a certain subfilter composition, has not been considered. This distinction is not unique to FDF and FPDF. It also needs to be considered for all other filtered quantities, such as the filtered velocities and the

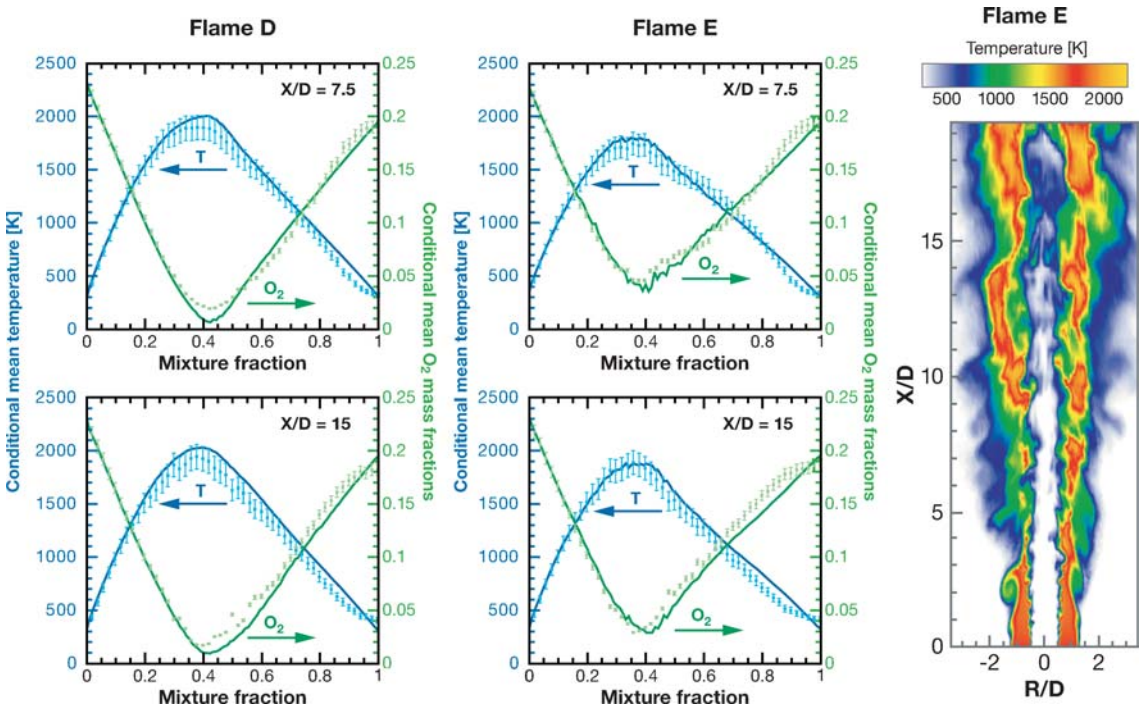

Figure 3

Results from large-eddy simulation of Sandia flame D and flame E (Raman & Pitsch 2005b) using the transported filtered density function model compared with experimental data of Barlow & Frank (1998). Comparison of mixture fraction–conditioned averages of temperature and O_2-mass fractions at $x/D = 7.5$ and $x/D = 15$ and temperature distribution (*right*). The extent of local extinction can be seen in the mass fraction of unburned O_2 at stoichiometric conditions ($Z_{st} = 0.35$) and is apparent in the instantaneous temperature field.

subfilter stress tensor. For these, however, this is usually done implicitly by modeling the unclosed subfilter terms in a statistical sense, which also implies that the filtered quantity obtained from the solution of the modeled equations has statistical meaning. Similarly, modeling of the mixing term in the FDF equation cannot be done for a single subfilter realization, but only for a statistical distribution on the subfilter scale. Therefore, to model the transport equation, it has to be written for the FPDF rather than the FDF.

3. LES OF PREMIXED TURBULENT COMBUSTION

3.1. Overview

Premixed turbulent combustion in technical devices often occurs in thin flame fronts. The propagation of these fronts, and hence also the heat release, is governed by the interaction of transport and chemistry within the front. In laminar flames, this strong

coupling is reflected in the scaling of the laminar burning velocity s_L, which can be expressed as $s_L \sim \sqrt{D/t_c}$, where D is the diffusion coefficient and t_c is a characteristic chemical timescale.

Different models have been proposed for LES of premixed turbulent combustion, most of which are variants of the flamelet concept (Colin et al. 2000, Hawkes & Cant 2000, Kim & Menon 2000, Knikker et al. 2002, Nottin et al. 2000, Pitsch & Duchamp de Lageneste 2002). Other models that have been proposed include the thickened flame model (Colin et al. 2000) and the linear eddy model (Chakravarthy & Menon 2001).

Much progress has been made over the past years in premixed combustion LES. However, one of the main roadblocks at present is that good, reliable, and comprehensive experimental data sets, adequately documented for use as validation data for LES, are very sparse. In particular, there is no equivalent to the standard validation experiments used for nonpremixed combustion (Barlow & Frank 1998, Dally et al. 1998). Because of this, models for premixed turbulent combustion are often not sufficiently validated. There is a need for good validation cases with comprehensive data sets at different Karlovitz numbers, varying from almost laminar to the broken reaction zones regime.

In the following, the premixed combustion regimes and their consequences for LES are first discussed. Next, the critical issue of flame resolution is addressed, and finally, the most commonly used models for turbulent premixed combustion LES are presented.

3.2. Regimes in Premixed Combustion LES

Regime diagrams are commonly used to characterize turbulence/flame interactions in premixed turbulent combustion. Different forms of regime diagrams have been proposed by Borghi (1985), Peters (1999), and others. Typically, the different regimes are presented in terms of u'/s_L and l_t/l_F, where u' and l_t are the characteristic velocity fluctuation and length scale of the large turbulent scales, and l_F is the laminar flame thickness. All these parameters are physical quantities, independent of the turbulence and combustion models used. A similar diagram could be constructed for LES using the filter size Δ as the length scale and the subfilter velocity fluctuation u'_Δ as the velocity scale. Such a representation introduces both physical and modeling parameters into the diagram. A change in the filter size, however, also leads to a change in the subfilter velocity fluctuation. This implies that the effect of the filter size, which is a numerical or model parameter, cannot be studied independently. In response to this issue, an LES regime diagram for characterizing subfilter turbulence/flame interactions in premixed turbulent combustion was proposed by Pitsch & Duchamp de Lageneste (2002), and recently extended by Pitsch (2005). This diagram is shown in **Figure 4**. In contrast to the RANS regime diagrams, Δ/l_F and the Karlovitz number Ka are used as the axes of the diagram. The Karlovitz number, defined as the ratio of the Kolmogorov timescale to the chemical timescale, describes the physical interaction of flow and combustion on the smallest turbulent scales. It is defined solely on the basis of physical quantities, and is hence independent of the filter size. The

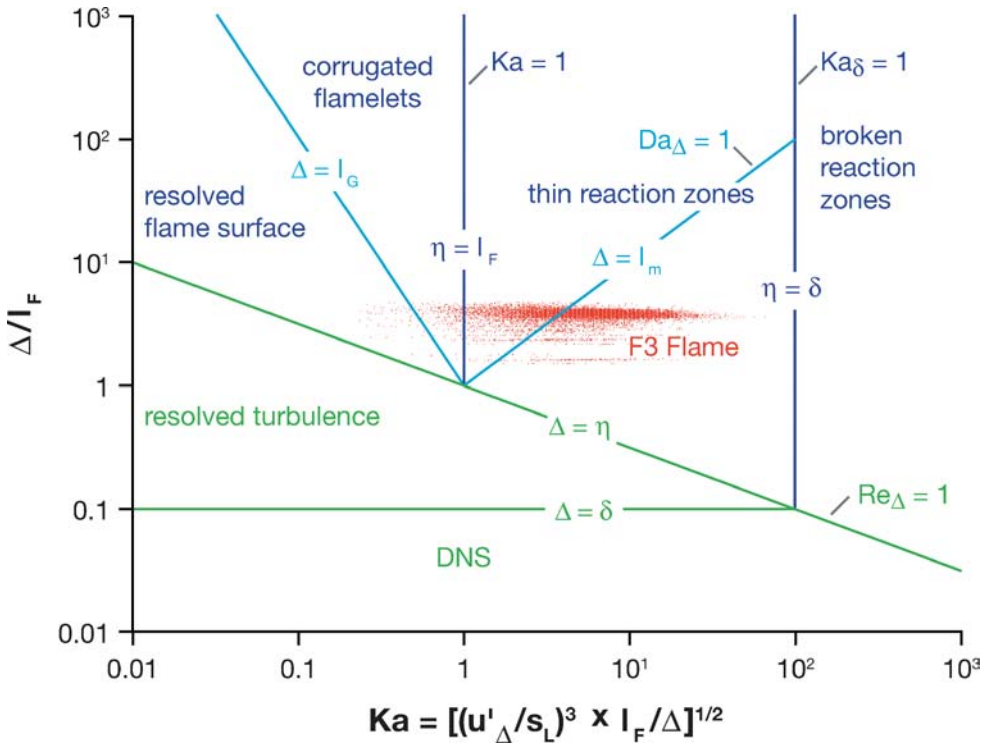

Figure 4

Regime diagram for large-eddy simulation (LES) and direct numerical simulation of premixed turbulent combustion (Pitsch 2005). Symbols show an instantaneous distribution of filter size and Ka number on the flame surface from LES of a premixed stoichiometric methane/air jet flame (Pitsch & Duchamp de Lageneste 2002). Conditions for the simulation correspond to flame F3 of Chen et al. (1996).

subfilter Reynolds and Damköhler numbers and the Karlovitz number relevant in the diagram are defined as

$$\mathrm{Re}_\Delta = \frac{u'_\Delta \Delta}{s_L l_F}, \qquad \mathrm{Da}_\Delta = \frac{s_L \Delta}{u'_\Delta l_F}, \quad \text{and} \quad \mathrm{Ka} = \frac{l_F^2}{\eta^2} = \left(\frac{u'^3_\Delta l_F}{s_L^3 \Delta}\right)^{1/2} \tag{7}$$

where η is the Kolmogorov scale.

In LES, the Karlovitz number is a fluctuating quantity, but for a given flow field and chemistry it is fixed. The effect of changes in filter size can therefore easily be assessed at constant Ka number. An additional benefit of this regime diagram is that it can be used equally well for DNS if Δ is associated with the mesh size. In the following, the physical regimes are briefly reviewed and relevant issues for LES are discussed.

The three regimes with essentially different interactions of turbulence and chemistry are the corrugated flamelet regime, the thin reaction zones regime, and the broken reaction zones regime. In the corrugated flamelet regime, the laminar

flame thickness is smaller than the Kolmogorov scale, and hence Ka $<$ 1. Turbulence will therefore wrinkle the flame, but will not disturb the laminar flame structure. In the thin reaction zones regime, the Kolmorogov scale becomes smaller than the flame thickness, which implies Ka $>$ 1. Turbulence then increases the transport within the chemically inert preheat region. In this regime, the reaction zone thickness δ is still smaller than the Kolmogorov scale. Because the reaction zone, which appears as a thin layer within the flame, can be estimated to be an order of magnitude smaller than the flame thickness, the transition to the broken reaction zones regime occurs at approximately Ka = 100. The thin reaction zone retains a laminar structure in the thin reaction zones regime, whereas the preheat region is governed by turbulent mixing, which enhances the burning velocity. In the broken reaction zones regime, the Kolmogorov scale becomes smaller than the reaction zone thickness. This implies that the Karlovitz number based on the reaction zone thickness, Ka_δ, becomes larger than one.

Most technical combustion devices are operated in the thin reaction zones regime, because mixing is enhanced at higher Ka numbers, which leads to higher volumetric heat release and shorter combustion times. The broken reaction zones regime is usually avoided in fully premixed systems. In this regime, mixing is faster than the chemistry, which leads to local extinction. This can cause noise, instabilities, and possibly global extinction. However, the broken reaction zones regime is significant, for instance, in partially premixed systems. In a lifted jet diffusion flame, the stabilization occurs by partially premixed flame fronts, which burn fastest at conditions close to stoichiometric mixture. Away from the stoichiometric surface toward the center of the jet, the mixture is typically very rich and the chemistry slow. Hence, the Ka number becomes large. This behavior has been found in the analysis of DNS results of a lifted hydrogen/air diffusion flame (Mizobuchi et al. 2002).

The effect of changing the LES filter width can be assessed by starting from any one of these regimes at large Δ/l_F. As the filter width is decreased, the subfilter Reynolds number, Re_Δ, eventually becomes smaller than one. Then the filter size is smaller than the Kolmogorov scale, and no subfilter modeling for the turbulence is required. However, the entire flame including the reaction zone is only resolved if $\Delta < \delta$.

In the corrugated flamelets regime, if the filter is decreased below the Gibson scale l_G, which is the smallest scale of the subfilter flame-front wrinkling, the flame-front wrinkling is completely resolved. It is apparent that in the corrugated flamelet regime, where the flame structure is laminar, the entire flame remains on the subfilter scale, if Δ/l_F is larger than one. This is always the case for LES.

In the thin reaction zones regime, the preheat region is broadened by the turbulence. Peters (1999) estimated the broadened flame thickness from the assumption that the timescale of the turbulent transport in the preheat zone has to be equal to the chemical timescale, which for laminar flames leads to the burning velocity scaling given in the beginning of this section. From this, the ratio of the broadened flame thickness l_m and the filter size can be estimated as (Pitsch 2005)

$$\frac{l_m}{\Delta} = \left(\frac{u'_\Delta l_F}{s_L \Delta}\right)^{3/2} = \mathrm{Ka}\frac{l_F}{\Delta} = \mathrm{Da}_\Delta^{-3/2}. \quad (8)$$

Hence, the flame is entirely on the subfilter scale as long as $Da_\Delta > 1$, and is partly resolved otherwise.

It is important to realize that the turbulence quantities, especially u'_Δ, and hence most of the nondimensional numbers used to characterize the flame/turbulence interactions, are fluctuating quantities and can significantly change in space and time. To give an example, the variation of these quantities from a specific turbulent stoichiometric premixed methane/air flame simulation is shown in **Figure 4**. This simulation was done for an experimental configuration with a nominal Ka number of Ka = 11, based on experimentally observed integral scales. The simulated conditions correspond to flame F3 of Chen et al. (1996), and details of the simulation can be found in Pitsch & Duchamp de Lageneste (2002). For a given point in time, the Ka number has been evaluated using appropriate subfilter models for all points on the flame surface. Because of the spatially varying filter size, but also because of heat losses to the burner, which locally lead to changes in l_F, there is a small scatter in Δ/l_F. Although the flame is mostly in the thin reaction zones regime, there is a strong variation in Ka number, ranging from the corrugated to the broken reaction zones regime.

3.3. Flame Resolution

One of the main challenges in premixed turbulent combustion LES is that for a substantial part of the regime diagram, the flame is entirely on the subfilter scale. Although the Da number and the filter width might be locally small enough to resolve the preheat region adequately, because of the large flow-field variations, there might always be substantial regions where the flame is under-resolved. In the example of the F3 premixed turbulent jet simulation indicated in the regime diagram shown in **Figure 4**, almost nowhere is the flame thickness large enough to be adequately resolved.

The fact that the flame often appears entirely on the subfilter scale is not a problem in itself. The temperature or progress variable fields can be filtered using a given filter width. The resulting filtered fields can then be discretized on an appropriate mesh, which would have a typical cell size approximately one order of magnitude smaller than the filter size. At present, however, this explicit filtering approach has never been used in combustion LES. The reasons are apparent. For the F3 flame, shown in **Figure 4**, the number of computational cells would have to be increased by one order of magnitude in each direction to resolve the filtered temperature field adequately.

If the flame occurs entirely on the subfilter scale, then for implicit filtering the change in temperature or progress variable from the unburned value to the burned value occurs essentially within one computational cell. This is certainly unacceptable from a numerical standpoint. Under-resolving the temperature jump will lead to numerical diffusion, which will enhance the burning velocity. The problem is similar to the challenge of computing shocks in supersonic flows, where a substantial amount of research has been devoted to develop accurate numerical algorithms. The added complexity for a turbulent flame, however, is that a flame does not always appear as a discontinuity, but can be substantially thicker than the filter size for high Ka number. In that case, some numerical algorithms designed for fronts might become unsuitable.

This issue must be properly dealt with by any model for premixed combustion LES, but is often neglected in the published work. Weller et al. (1998), for instance, proposed and applied a model based on the solution of an unburned gas mass fraction transport equation in the flamelet regime without considering the front discontinuity. Conversely, other models have been specifically devised with the flame resolution in mind. In the thickened flame model by Colin et al. (2000), chemistry/transport interaction is artificially modified to obtain a thickened flame that can be resolved on a given mesh. To achieve this, the turbulent transport coefficient is multiplied by a constant factor. Then, to obtain the same flame speed as in the unmodified case, the chemical source term is divided by the same factor. The source term is further empirically modified by a so-called efficiency function that has been determined from DNS of flame/vortex interactions. Although this method resolves the artificial flame, the flame/turbulence interaction has to be changed from a transport-controlled to a chemistry-controlled combustion regime, and the effect of the heat release on the flow field cannot be described adequately.

A possible and appropriate, but quite complex, solution is to use explicit filtering and ensure resolution of the flame using adaptive local mesh refinement. Another viable approach that avoids the discontinuity altogether is the *G*-equation model, which is discussed below.

3.4. Models for Premixed Turbulent Combustion

The laminar flamelet model is the prevalent model for premixed turbulent combustion LES. It has been extensively used in RANS and many model formulations have been proposed based on the flamelet concept (Bray et al. 1984, 1985; Peters 1992, 1999; Trouvé & Poinsot 1994). The only other models that have been applied in LES of premixed combustion are the thickened flame model, which has been briefly described above and the linear eddy model (Chakravarthy & Menon 2001). A discussion of the two most widely used formulations follows.

3.4.1. Flame-surface density models. In premixed turbulent combustion, the reaction progress variable is often used as a representative reactive scalar. It can be defined as a normalized temperature or reaction product mass fraction. The normalization is such that the reaction progress variable is zero in the unburned gases and unity for equilibrium conditions. A filtered form of the transport equation of the reaction progress variable can be derived easily. This equation has three unclosed terms: the subfilter scalar flux term, the filtered molecular transport, and the filtered chemical source term.

The proposed models for these terms in LES are mostly very similar to the respective RANS models (Boger et al. 1998, Hawkes & Cant 2000). The general idea of the flame-surface density model is that the volumetric consumption rate of the unburned gases is essentially given by the product of the flame-surface and the flame-propagation speed. Hence, the filtered molecular transport and chemical source terms are jointly modeled as a propagation term proportional to the subfilter flame-surface density (FSD), which expresses the flame surface per unit volume. A transport

equation for the FSD was first derived by Pope (1988), and several different closure models have been provided for RANS (e.g., Trouvé & Poinsot 1994). The FSD can be computed by solving the modeled transport equation. Alternatively, the assumption that production equals dissipation in the transport equation leads to an algebraic model. FSD models for LES were first investigated by Boger et al. (1998). Hawkes & Cant (2000) provided an FSD formulation that is similar to the typical RANS models in the subfilter terms, but which includes the resolved contributions, typically neglected for RANS. This model therefore satisfies the DNS limit for fully resolved simulations.

The subfilter scalar flux is often modeled using gradient transport models. However, for premixed turbulent combustion, in many experiments and DNS results, especially for weak turbulence, the heat release causes so-called counter-gradient diffusion. Therefore, the typical gradient transport models are generally not applicable (Kalt et al. 1998, Veynante et al. 1997). Subfilter scalar flux models for the reaction progress variable in premixed combustion LES that address this issue have been proposed, for instance, by Hawkes & Cant (2000) and Tullis & Cant (2003).

For the FSD model, the reaction progress variable equation always has to be solved, which for Da $>$ 1 cannot be done in LES without special treatment of the discontinuity. For the FSD itself, this problem does not arise as long as an algebraic model is used. If, however, an FSD transport equation is solved, the problem is amplified, because the FSD is only nonzero in regions where the filtered reaction progress variable changes from zero to one, which is on the order of the filter size.

3.4.2. *G*-Equation model. The *G*-equation model for premixed turbulent combustion, originally proposed by Williams (1985), is another variant of the flamelet model. The flame-front position is represented with a constant value G_0 of the level set function G. The value of G away from the front is arbitrary within some limits, but is typically chosen to be a signed distance function so that $G = 0$ at the front, $G < 0$ in the unburned mixture, and $G > 0$ in the burned gases. The surface represented by the level set function can be chosen to be a surface of constant temperature, reaction progress variable, or other similar quantity. The assumption of an infinitely thin flame is not required. In this sense, the *G*-equation approach is not a model, but merely a numerical method that is suited to overcome the problem of flame resolution described above. As for the reaction progress variable equation, closure for a *G*-equation describing the mean evolution of the flame front is still required. This has been provided for Reynolds averaging by Peters (1992, 1999), and applications are presented in the literature (Chen et al. 2000, Peters 2000).

Oberlack et al. (2001) showed that compared with the reaction progress variable equation, the *G*-equation has a special symmetry, the so-called generalized scaling symmetry, which has the consequence that the value of G used to represent the flame front is arbitrary. Oberlack et al. (2001) argued that because of this property, the classical way of Reynolds ensemble averaging of the *G*-field cannot be performed. New averaging techniques that are consistent with the special character of the *G*-equation have been proposed by Peters (2000) and Oberlack et al. (2001). These averaging

procedures only consider the instantaneous flame surface in the definition of a mean flame-front location. Another implication of the generalized scaling symmetry is that the modeled equation cannot have a diffusion or turbulent transport term, which typically appears in the equation for the reaction progress variable. Consequently, Peters (1999) modeled the scalar flux term, appearing in his derivation of the mean *G*-equation, as a curvature term.

LES formulations of the *G*-equation method have been proposed by several authors (Huang et al. 2003, Kim & Menon 2000, Pitsch & Duchamp de Lageneste 2002). However, the proposed forms of the *G*-equation for the filtered flame-front position did not consider the special character of the *G*-equation in the derivation. This led to formulations that are inconsistent with the generalized scaling symmetry. A consistent formulation based on a new filtering technique was only recently provided (Pitsch 2005). Based on the new filter, the *G*-equation for the filtered flame-front position valid in the corrugated flamelets and the thin reaction zones regime was derived as

$$\frac{\partial \check{G}}{\partial t} + \hat{\boldsymbol{v}} \cdot \nabla \check{G} = -(s_L + s_\kappa)\,\mathbf{n} \cdot \nabla \check{G}. \tag{9}$$

Here, $\mathbf{n}$ is the flame-front normal vector, and s_L and s_κ describe laminar flame propagation and flame advancement by curvature effects, respectively. Note that the $\widehat{\ }$-symbol denotes a filtering operation, whereas the $\check{\ }$-symbol does not. $\check{G}$ is not the filtered *G*-field, but a level set representation of the filtered flame-front position.

The equation has two unclosed terms, a flame-front-conditioned filtered velocity and a propagation term. For the conditional velocity, a model in terms of the unconditionally Favre-filtered velocity was provided (Pitsch 2005). For the propagation term, the following form was proposed:

$$(s_L + s_\kappa)\,\mathbf{n} = (\widehat{s_L} - D\check{\kappa} + s_T - D_{t,\kappa}\check{\kappa})\,\check{\mathbf{n}}. \tag{10}$$

The first two terms in the model describe the resolved parts of the burning velocity, which ensure that the instantaneous equation is recovered in the resolved turbulence regime shown in **Figure 4**. The third term represents the subfilter contributions from the corrugated flamelets and the thin reaction zones regime. Because this term is entirely on the subfilter scale, it can be modeled in analogy to the RANS model. Following Oberlack et al. (2001), an equation for a length scale representing the subfilter flame brush thickness can be derived. Closure of the production and dissipation terms using the arguments of Peters (1999), and assuming a balance of production and dissipation on the subfilter level leads to an algebraic relation for s_T. It can be expected, and has been shown by Hawkes & Cant (2001), that the subfilter flame brush thickness is on the order of the filter width Δ. For constant filter width, the temporal change and transport of this quantity should therefore be small. Hence, compared with the RANS models, the production/dissipation balance assumption seems to be better justified for LES. However, this assumption might fail close to a nozzle or flame holder, where the flame is still not fully established.

The last term accounts for the interaction of subfilter turbulent transport with the resolved flame-front curvature. Note that the diffusivity in this equation is not

necessarily equal to the subfilter diffusivity. Peters (1999) argued that turbulent mixing in the preheat region occurs by turbulent eddies of a characteristic length l_m. According to Equation 8, these eddies are smaller than Δ if Da $>$ 1. The diffusivity $D_{t,\kappa}$ appearing in Equation 10 is then given by $D_{t,\kappa} = D_t \mathrm{Da}_\Delta^{-2}$. For Da $<$ 1, mixing in the preheat zone is partly resolved and the sub-filter contribution is $D_{t,\kappa} = D_t$.

One modeling challenge that is unique to the *G*-equation is that the flame is only represented by a surface. Even in the thin reaction zones regime, where the flame is broadened by turbulence, the flame structure is not resolved and has to be modeled in the computation of density and other quantities of interest. This is less important if $\mathrm{Da}_\Delta > 1$, because the flame is entirely on the subfilter scale, but becomes important otherwise. In addition, for using the *G*-equation in LES, the accuracy of numerical schemes used for advection and the so-called reinitialization process, are particularly important.

4. LES OF REAL COMBUSTION DEVICES

Several investigators have reported simulations of real combustion devices with LES. Most of these use either structured or block-structured curvi-linear meshes, which cannot deal with very complex geometries. Simulations of gas turbines, for instance, typically require unstructured meshing strategies, for which the formulation of energy conserving and accurate numerical algorithms, of particular importance for combustion LES, proves to be even more difficult. Among the few fully unstructured multiphysics LES codes are the AVBP code of CERFACS, which has been applied in many studies on combustion instabilities and flashback in premixed gas turbines (Selle et al. 2004, Sommerer et al. 2004), and the Stanford CDP code.[1] CDP solves both low-Ma number variable-density and fully compressible LES equations using the unstructured collocated finite volume discretization of Mahesh et al. (2004) and its subsequent improvements by Ham & Iaccarino (2004). It applies Lagrangian particle tracking with adequate models for breakup, particle drag, and evaporation for liquid fuel sprays. Closure for subfilter transport terms and other turbulence statistics is accomplished using dynamic models. The FPV combustion model, described in section 2.3.2, is applied to model turbulence/chemistry interactions. The code is parallelized with advanced load balancing procedures for both gas and particle phases. Computations have been conducted with over two billion cells using several thousand processors.

A state-of-the-art simulation of a section of a modern Pratt & Whitney gas turbine combustor that uses all these capabilities has been performed (Mahesh et al. 2005, Moin & Apte 2005) and is shown in **Figure 5**. The figure shows the spray and temperature distribution and demonstrates the complexity of the geometry and the associated flow physics.

[1] CDP is named after the late Charles D. Pierce (1969–2002), who was one of the early pioneers of combustion LES.

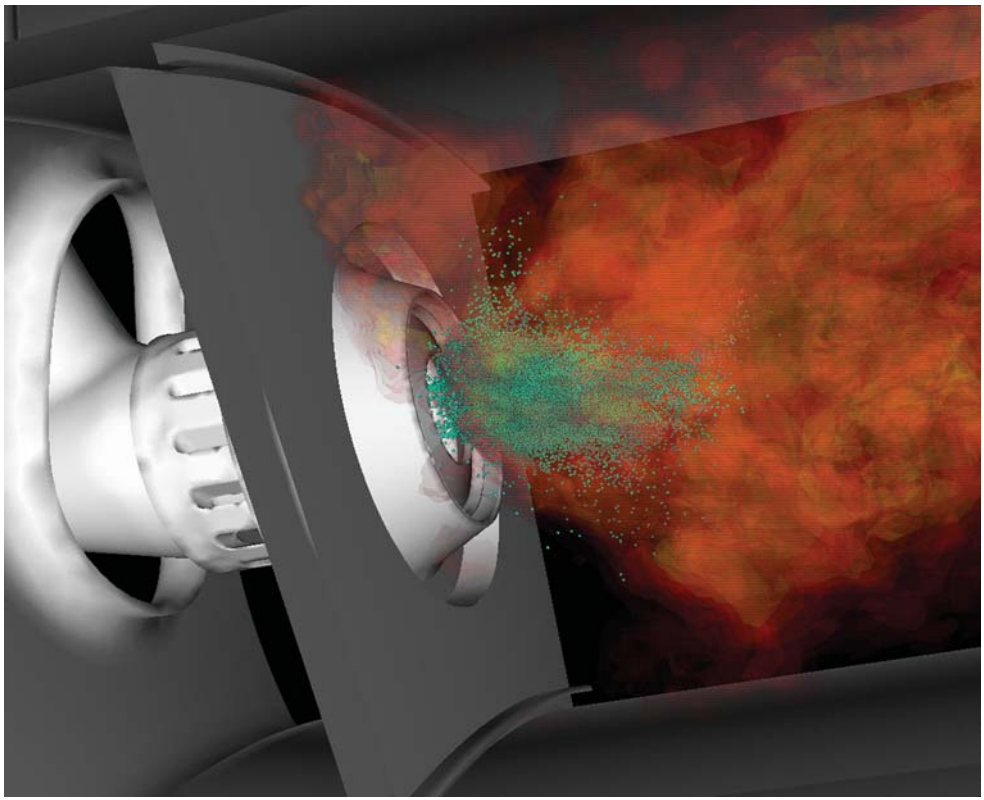

Figure 5

Large-eddy simulation of a modern Pratt & Whitney gas turbine combustor (Mahesh et al. 2005, Moin & Apte 2005). The combustor bulkhead is to the left of the flame. Fuel and air enter the combustor through the injector/swirler assembly, which has three different air passages. Fuel droplets are shown in green. The remaining color representation shows iso-surfaces of the temperature. Dilution by secondary air occurs to the right of the figure and is not shown.

5. CONCLUSIONS

Combustion LES appeared in the literature only a little more than a decade ago. Many studies have been performed in a priori testing and simulations of academic configurations as well as practical combustion devices exploring the potential of combustion LES. But compared to the richness of the field, little fundamental research has been done that goes beyond the methods typically applied in the Reynolds-averaged context. Some of the outstanding exceptions are discussed in this paper. It is argued and demonstrated that LES clearly offers advantages that move the state of the art toward accurate and predictive simulations of turbulent combustion.

The tremendous recent advancements in experimental techniques (Barlow & Frank 1998, Dally et al. 1998, Karpetis & Barlow 2002, Schneider et al. 2003) for simultaneous measurements of scalar quantities provide joint one-point and multipoint

statistics of species mass fractions in turbulent nonpremixed jet flames. These data have opened a path for more detailed validation studies, but also for a priori testing of subfilter models using experimental data. Still, for further model development, more such data are needed in more complex flow environments and confined flows. Just as the Sandia flame experiments are now the prime validation data for nonpremixed combustion, a database for premixed combustion should be established. For nonpremixed combustion, it is clear that the desired data include mixture fraction–conditioned averages and PDFs. However, for premixed turbulent combustion, the desired quantities have yet to be defined. These could, for example, include flame topology, burning velocity, and species mass fractions and velocity fields conditioned on a well-defined reaction progress variable.

In the future, some common practices of combustion LES have to be revisited. For nonpremixed combustion, it has been pointed out that the models for the scalar dissipation rate and the scalar variance need to be improved, the feasibility of unsteady flamelet models and CMC in LES of practical systems has to be demonstrated, and for transported FDF/LES methods, mixing models and computational efficiency have to be improved. Especially for premixed combustion, more detailed validation of the models is required.

The importance of accurate and kinetic energy–conserving numerical schemes in LES has been noted many times (Mahesh et al. 2004, Rogallo & Moin 1984), but it is often argued that for many applications of LES the error introduced by only using second-order numerical schemes is small compared with modeling errors. For combustion LES, where the subfilter scales, and hence also the energy contained in these scales, is of great importance, this assumption has to be revisited. Similarly, the effects of explicit versus implicit filtering need to be assessed. Althought many fundamental questions still have to be addressed, it has been demonstrated that combustion LES can be applied for computations involving complex geometry and multiphase flows. Combustion LES is on the verge of being used in the design cycle of engines and other combustion devices, but more validation of the methods for complex systems is needed.

ACKNOWLEDGMENTS

Funding of the author's work was provided by the Department of Energy within the ASC program and the Air Force Office of Scientific Research. The author thanks Dr. Venkat Raman and Dr. Marcus Herrmann for valuable comments and many inspiring discussions.

LITERATURE CITED

Angelberger C, Veynante D, Egolfopoulos F. 2000. LES of chemical and acoustic forcing of a premixed dump combustor. *Flow Turbul. Combust.* 65(2):205–22

Barlow RS, ed. 2000. *Proc. Fifth Int. Workshop Meas. Comput. Turbulent Nonpremixed Flames*

Barlow RS, Frank JH. 1998. Effect of turbulence on species mass fractions in methane/air jet flames. *Proc. Combust. Inst.* 27:1087–95

Bilger RW. 1976. The stucture of diffusion flames. *Combust. Sci. Technol.* 13:155

Bilger RW. 1993. Conditional moment closure for turbulent reacting flow. *Phys. Fluids A* 5:436–44

Bilger RW, Pope SB, Bray KNC, Driscoll JF. 2005. Paradigms in turbulent combustion research. *Proc. Comb. Inst.* 30:21–42

Boger M, Veynante D, Boughanem H, Trouvé A. 1998. Direct numerical simulation analysis of flame surface density concept for large eddy simulation of turbulent premixed combustion. *Proc. Combust. Inst.* 27:917–25

Borghi R. 1985. On the structure and morphology of turbulent premixed flames. In *Recent Advances in the Aerospace Science*, ed. C Casci, pp. 117–38. New York: Plenum

Bowman CT, Hanson RK, Davidson DF, Gardiner WC Jr, Lissianski V, et al. 1995. *Gri-mech 2.11.* **http://www.me.berkeley.edu/gri_mech/**

Branley N, Jones W. 2001. Large eddy simulation of a turbulent non-premixed flame. *Combust. Flame* 127(1-2):1914–34

Bray KNC, Libby PA, Moss JB. 1984. Flamelet crossing frequencies and mean reaction rates in premixed turbulent combustion. *Combust. Sci. Technol.* 41:143–72

Bray KNC, Libby PA, Moss JB. 1985. Unified modeling approach for premixed turbulent combustion. 1. General formulation. *Combust. Flame* 61:87–102

Bushe WK, Steiner H. 1999. Conditional moment closure for large eddy simulation of nonpremixed turbulent reacting flows. *Phys. Fluids* 11:1896–906

Chakravarthy VK, Menon S. 2001. Large-eddy simulation of turbulent premixed flames in the flamelet regime. *Combust. Sci. Technol.* 162:175

Chen JY, Kollman W, Dibble RW. 1989. PDF modeling of turbulent methane-air nonpremixed jet flames. *Combust. Sci. Technol.* 64:315–46

Chen M, Herrmann M, Peters N. 2000. Flamelet modeling of lifted turbulent methane/air and propane/air jet diffusion flames. *Proc. Combust. Inst.* 28:167–74

Chen YC, Peters N, Schneemann GA, Wruck N, Renz U, Mansour MS. 1996. The detailed flame structure of highly stretched turbulent premixed methane-air flames. *Combust. Flame* 107:233–44

Colin F, Veynante D, Poinsot T. 2000. A thickened flame model for large eddy simulation of premixed turbulent combustion. *Phys. Fluids* 12(7):1843–63

Colucci PJ, Jaberi FA, Givi P, Pope SB. 1998. Filtered density function for large eddy simulation of turbulent reacting flows. *Phys. Fluids* 10:499–515

Cook AW, Riley JJ. 1994. A subgrid model for equilibrium chemistry in turbulent flows. *Phys. Fluids* 6:2868–70

Cook AW, Riley JJ. 1998. Subgrid-scale modeling for turbulent reactive flows. *Combust. Flame* 112:593–606

Dally BB, Masri AR, Barlow RS, Fietchner GJ. 1998. Instantaneous and mean compositional structure of bluff-body stabilized nonpremixed flames. *Combust. Flame* 114:119–48

De Bruyn Kops SM, Riley JJ, Kosaly G, Cook AW. 1998. Investigation of modeling for non-premixed turbulent combustion. *Flow Turbul. Combust.* 60:105–22

Di Mare F, Jones W, Menzies K. 2004. Large eddy simulation of a model gas turbine combustor. *Combust. Flame* 137(3):278–94

Eggenspieler G, Menon S. 2004. Large-eddy simulation of pollutant emission in a DOE-HAT combustor. *J. Propuls. Power* 20(6):1076–85

Fox RO. 2003. *Computational Models for Turbulent Reacting Flows*. Cambridge, UK: Cambridge Univ. Press

Gao F, O'Brien EE. 1993. A large-eddy simulation scheme for turbulent reacting flows. *Phys. Fluids A* 5:1282–84

Germano M, Piomelli U, Moin P, Cabot WH. 1991. A dynamic subgrid-scale eddy viscosity model. *Phys. Fluids A* 3(7):1760–65

Girimaji SS, Zhou Y. 1996. Analysis and modeling of subgrid scalar mixing using numerical data. *Phys. Fluids* 8:1224–36

Ham F, Iaccarino G. 2004. Energy conservation in collocated discretization schemes on unstructured meshes. In *CTR Annual Research Briefs*. Stanford, CA: Center for Turbulence Research, NASA Ames/Stanford Univ.

Hawkes E, Cant R. 2001. Physical and numerical realizability requirements for flame surface density approaches to large-eddy and Reynolds averaged simulation of premixed turbulent combustion. *Combust. Theory Model.* 5(4):699–720

Hawkes ER, Cant RS. 2000. A flame surface density approach to large-eddy simulation of premixed turbulent combustion. *Proc. Combust. Inst.* 28:51–58

Haworth D, Jansen K. 2000. Large-eddy simulation on unstructured deforming meshes: towards reciprocating IC engines. *Comput. Fluids* 29(5):493–524

Huang Y, Sung H, Hsieh S, Yang V. 2003. Large-eddy simulation of combustion dynamics of lean-premixed swirl-stabilized combustor. *J. Propuls. Power* 19(5):782–94

Ihme M, Cha CM, Pitsch H. 2005. Prediction of local extinction and re-ignition effects in non-premixed turbulent combustion by a flamelet/progress variable approach. *Proc. Combust. Inst.* 30:793–800

Ihme M, Pitsch H. 2005. LES of a non-premixed flame using an extended flamelet/progress variable model. *AIAA Pap.* 2005-0558

Janicka J, Sadiki A. 2005. Large eddy simulation of turbulent combustion systems. *Proc. Combust. Inst.* 30:537–47

Jiménez C, Ducros F, Cuenot B, Bédat B. 2001. Subgrid scale variance and dissipation of a scalar field in large eddy simulations. *Phys. Fluids* 13(6):1748–54

Jimenez J, Linan A, Rogers MM, Higuera FJ. 1997. A priori testing of subgrid models for chemically reacting non-premixed turbulent shear flows. *J. Fluid Mech.* 349:149–71

Kalt PAM, Frank JH, Bilger RW. 1998. Laser imaging of conditional velocities in premixed propane-air flames by simultaneous OH PLIF and PIV. *Proc. Combust. Inst.* 27:751–58

Karpetis AN, Barlow RS. 2002. Measurements of scalar dissipation in a turbulent piloted methane/air jet flame. *Proc. Combust. Inst.* 29:1929–36

Kempf A, Sadiki A, Janicka J. 2003. Prediction of finite chemistry effects using large eddy simulation. *Proc. Combust. Inst.* 29:1979–85

Kim SH, Huh KY. 2002. Use of conditional moment closure model to predict NO formation in a turbulent CH_4/H_2 flame over a bluff-body. *Combust. Flame* 130(1–2):94–111
Kim SH, Pitsch H. 2005. Conditional filtering method for large eddy simulation of turbulent nonpremixed combustion. *Phys. Fluids* In press
Kim W, Menon S, Mongia H. 1999. Large-eddy simulation of a gas turbine combustor flow. *Combust. Sci. Technol.* 143(1–6):25
Kim WW, Menon S. 2000. Numerical modeling of turbulent premixed flames in the thin-reaction-zones regime. *Combust. Sci. Technol.* 160:119–50
Klimenko AY. 1990. Multicomponent diffusion of various scalars in turbulent flow. *Fluid Dyn.* 25:327–34
Klimenko AY, Bilger RW. 1999. Conditional moment closure for turbulent combustion. *Prog. Energy Combust. Sci.* 25:595–687
Knikker R, Veynante D, Meneveau C. 2002. A priori testing of a similarity model for large eddy simulations of turbulent premixed combustion. *Proc. Combust. Inst.* 29:2105–11
Lesieur M, Métais O. 1996. New trends in large-eddy simulations of turbulence. *Annu. Rev. Fluid Mech.* 28:45–82
Lu L, Ren Z, Raman V, Pope S, Pitsch H. 2004. LES/FDF/ISAT computations of turbulent flames. In *Proc. 2004 CTR Summer Program*, pp. 283–94. Cent. Turbul. Res., NASA Ames/Stanford Univ.
Maas U, Pope S. 1992. Simplifying chemical kinetics: Intrinsic low-dimensional manifolds in composition space. *Combust. Flame* 88:239–64
Mahesh K, Constantinescu G, Apte S, Iaccarino G, Ham F, Moin P. 2005. Large-eddy simulation of reacting turbulent flows in complex geometriers. *ASME J. Appl. Mech.* In press
Mahesh K, Constantinescu G, Moin P. 2004. A numerical method for large-eddy simulation in complex geometries. *J. Comp. Phys.* 197:215–40
Meneveau C, Katz J. 2000. Scale-invariance and turbulence models for large-eddy simulation. *Annu. Rev. Fluid Mech.* 32:1–32
Mizobuchi Y, Tachibana S, Shinio J, Ogawa S, Takeno T. 2002. A numerical analysis of the structure of a turbulent hydrogen jet lifted flame. *Proc. Combust. Inst.* 29:2009–15
Moin P. 2002. Advances in large eddy simulation methodology for complex flows. *Int. J. Heat Fluid Flow* 23(5):710–20
Moin P. 2004. Large eddy simulation of multi-phase turbulent flows in realistic combustors. *Prog. Comput. Fluid Dyn.* 4(3–5):237–40
Moin P, Apte S. 2005. Large-eddy simulation of realistic gas turbine combustors. *AIAA J.* In press
Moin P, Squires K, Cabot W, Lee S. 1991. A dynamic subgrid-scale model for compressible turbulence and scalar transport. *Phys. Fluids A* 3:2746–57
Muradoglu M, Jenny P, Pope SB, Caughey DA. 1999. A consistent hybrid finite-volume/particle method for the PDF equations of turbulent reactive flows. *J. Comput. Phys.* 154:342–71
Muradoglu M, Liu K, Pope SB. 2003. PDF modeling of a bluff-body stabilized turbulent flame. *Combust. Flame* 132(1–2):115–37

Nottin C, Knikker R, Boger M, Veynante D. 2000. Large-eddy simulation of an acoustically excited turbulent premixed flame. *Proc. Combust. Inst.* 28:67–73
Oberlack M, Wenzel H, Peters N. 2001. On symmetries and averaging of the *G*-equation for premixed combustion. *Combust. Theory Model.* 5(4):1–20
Peters N. 1983. Local quenching due to flame stretch and non-premixed turbulent combustion. *Combust. Sci. Technol.* 30:1–17
Peters N. 1984. Laminar diffusion flamelet models in non-premixed turbulent combustion. *Prog. Energy Combust. Sci.* 10:319–39
Peters N. 1992. A spectral closure for premixed turbulent combustion in the flamelet regime. *J. Fluid Mech.* 242:611–29
Peters N. 1999. The turbulent burning velocity for large scale and small scale turbulence. *J. Fluid Mech.* 384:107–32
Peters N. 2000. *Turbulent Combustion*. Cambridge, UK: Cambridge Univ. Press
Peters N, Williams FA. 1987. The asymptotic structure of stoichiometric methane-air flames. *Combust. Flame* 68:185–207
Pierce CD, Moin P. 1998. A dynamic model for subgrid-scale variance and dissipation rate of a conserved scalar. *Phys. Fluids* 10:3041–44
Pierce CD, Moin P. 2001. Progress-variable approach for large eddy simulation of turbulent combustion. *Rep. TF80, Flow Physics and Computation Division*, Dept. Mech. Eng., Stanford Univ.
Pierce CD, Moin P. 2004. Progress-variable approach for large eddy simulation of non-premixed turbulent combustion. *J. Fluid Mech* 504:73–97
Pitsch H. 2002. Improved pollutant predictions in large-eddy simulations of turbulent non-premixed combustion by considering scalar dissipation rate fluctuations. *Proc. Combust. Inst.* 29:1971–78
Pitsch H. 2005. A consistent level set formulation for large-eddy simulation of premixed turbulent combustion. *Combust. Flame* In press
Pitsch H, Chen M, Peters N. 1998. Unsteady flamelet modeling of turbulent hydrogen/air diffusion flames. *Proc. Combust. Inst.* 27:1057–64
Pitsch H, Duchamp de Lageneste L. 2002. Large-eddy simulation of premixed turbulent combustion using a level-set approach. *Proc. Combust. Inst.* 29:2001–8
Pitsch H, Ihme M. 2005. An unsteady/flamelet progress variable method for LES of nonpremixed turbulent combustion. *AIAA Pap. 2004-557*
Pitsch H, Peters N. 1998. A consistent flamelet formulation for non-premixed combustion considering differential diffusion effects. *Combust. Flame* 114:26–40
Pitsch H, Steiner H. 2000a. Large-eddy simulation of a turbulent piloted methane/air diffusion flame (Sandia flame D). *Phys. Fluids* 12(10):2541–54
Pitsch H, Steiner H. 2000b. Scalar mixing and dissipation rate in large-eddy simulations of non-premixed turbulent combustion. *Proc. Combust. Inst.* 28
Pope S. 1979. A rational method of determining probability distributions in turbulent reacting flows. *J. Non-Equilib. Thermodyn.* 4:309–20
Pope SB. 1985. PDF methods for turbulent reactive flows. *Prog. Energy Combust. Sci.* 11:119
Pope SB. 1988. The evolution of surfaces in turbulence. *J. Eng. Sci.* 26:445–69
Pope SB. 1990. Computations of turbulent combustion: progress and challenges. *Proc. Combust. Inst.* 23:591–612

Pope S. 1997. Computationally efficient implementation of combustion chemistry using in situ adaptive tabulation. *Combust. Theory Model.* 1:41–63
Pope S. 2004. Ten questions concerning the large-eddy simulation of turbulent flows. *N. J. Phys.* 6:35
Raman V, Pitsch H. 2005. Large-eddy simulation of a bluff-body stabilized non-premixed flame using a recursive-refinement procedure. *Combust. Flame* 142:329–47
Raman V, Pitsch H, Fox RO. 2005. Hybrid large-eddy simulation/Lagrangian filtered density function approach for simulating turbulent combustion. *Combust. Flame* In press
Rogallo RS, Moin P. 1984. Numerical simulation of turbulent flows. *Annu. Rev. Fluid Mech.* 16:99–137
Saxena V, Pope SB. 1998. PDF calculations of major and minor species in a turbulent piloted jet flame. *Proc. Combust. Inst.* 27:1081–86
Schneider C, Dreizler A, Janicka J, Hassel E. 2003. Flow field measurements of stable and locally extinguishing hydrocarbon-fuelled jet. *Combust. Flame* 135:185–90
Selle L, Lartigue G, Poinsot T, Koch R, Schildmacher K, et al. 2004. Compressible large eddy simulation of turbulent combustion in complex geometry on unstructured meshes. *Combust. Flame* 137(4):489–505
Sheikhi MRH, Drozda TG, Givi P, Jaberi FA, Pope SB. 2005. Large eddy simulation of a turbulent nonpremixed piloted methane jet flame (Sandia flame D). *Proc. Comb. Inst.* 30:549–56
Sheikhi MRH, Drozda TG, Givi P, Pope SB. 2003. Velocity-scalar filtered density function for large eddy simulation of turbulent flows. *Phys. Fluids* 15(8):2321–37
Shinjo J, Mizobuchi Y, Ogawa S. 2003. LES of unstable combustion in a gas turbine combustor. *High Perform. Comput.* 2858:234–44
Sommerer Y, Galley D, Poinsot T, Ducruix S, Lacas F, Veynante D. 2004. Large eddy simulation and experimental study of flashback and blow-off in a lean partially premixed swirled burner. *J. Turb.* 5:037
Sripakagorn P, Mitarai S, Kosály G, Pitsch H. 2004. Extinction and reignition in a diffusion flame (a direct numerical simulation study). *J. Fluid Mech.* 518:231–59
Stone C, Menon S. 2003. Open-loop control of combustion instabilities in a model gas turbine combustor. *J. Turbul.* 4:020
Tong C. 2001. Measurements of conserved scalar filtered density function in a turbulent jet. *Phys. Fluids* 13(10):2923–37
Tong C, Wang D, Barlow RS, Karpetis AN. 2005. Investigation of scalar filtered mass density function in turbulent partially premixed flames. *Jt. Meet. U.S. Sect. Combust. Inst., E23, Philadelphia, PA*
Trouvé A, Poinsot T. 1994. The evolution equation for the flame surface density in turbulent premixed combustion. *J. Fluid Mech* 278:1–31
Tullis S, Cant R. 2003. Scalar transport modeling in large eddy simulation of turbulent premixed flames. *Proc. Combust. Inst.* 29:2097–104
Veynante D, Trouvé A, Bray KNC, Mantel T. 1997. Gradient and countergradient scalar transport in turbulent premixed flames. *J. Fluid Mech* 332:263–93
Veynante D, Vervisch L. 2002. Turbulent combustion modeling. *Prog. Energy Combust. Sci.* 28(3):193–266

Wall C, Boersma B, Moin P. 2000. An evaluation of the assumed beta PDF subgrid-scale model for LES of non-premixed, turbulent combustion with heat release. *Phys. Fluids* 12(10):2522–29

Wall CT, Moin P. 2005. Numerical methods for large eddy simulation of acoustic combustion instabilities. *Tech. Rep. TF-91*. Stanford, CA: Stanford Univ.

Weller HG, Tabor G, Gosman AD, Fureby C. 1998. Application of a flame-wrinkling LES combustion model to a turbulent mixing layer. *Proc. Combust. Inst.* 27:899–907

Williams FA. 1985. Turbulent combustion. In *The Mathematics of Combustion*, ed. JD Buckmaster, pp. 197–1318. Soc. Ind. Appl. Math.

Xu J, Pope SB. 2000. PDF calculations of turbulent nonpremixed flames with local extinction. *Combust. Flame* 123:281–307

Zhang Y, Haworth D. 2004. A general mass consistency algorithm for hybrid particle/finite-volume PDF methods. *J. Comp. Phys.* 194(1):156–93